

Microcavities in polymeric photonic crystals

Hong-Bo Sun and Vygantas Mizeikis

Satellite Venture Business Laboratory, The University of Tokushima, 2-1 Minamijyosanjima, Tokushima 770-8506, Japan

Ying Xu, Saulius Juodkazis, Jia-Yu Ye, Shigeki Matsuo, and Hiroaki Misawa^{a)}

Department of Ecosystem Engineering, Graduate School of Engineering, The University of Tokushima, 2-1 Minamijyosanjima, Tokushima 770-8506, Japan

(Received 12 February 2001; accepted for publication 2 May 2001)

We report the fabrication and characteristics of planar microcavities in a log-pile photonic crystal structure formed using light-induced photopolymerization of resin. A planar defect was introduced into the middle of the log-pile structure as a single layer with every second rod missing. The existence of confined cavity states was confirmed experimentally and by numeric simulations. The cavity resonance found at the midgap wavelength $\lambda_M \sim 4.0 \mu\text{m}$ had a quality factor of about 130.

© 2001 American Institute of Physics. [DOI: 10.1063/1.1381035]

The possibility of controlling light emission and propagation using photonic crystal (PhC) structures has attracted much interest in the past decade. Embedding an optically active medium into a PhC structure inhibits light emission into undesired modes,^{1,2} and allows the realization of highly efficient optical emitters, such as light emitting diodes (LEDs) and thresholdless laser diodes (LDs). The essential requirement for the realization of these, as well as for many other PhC-based devices, is the ability to form PhC microcavities by introducing defects into their periodic structures.

So far, most successful PhC structures have been fabricated in semiconductors,³⁻⁵ since semiconductor processing techniques provide the most advanced tools for the fabrication of nanometric structures. To mention just a few examples, line,⁴ air-bridge,³ and bent waveguides⁵ as well as low-threshold lasing⁶ have been reported. Simultaneous with the development of semiconductor PhC structures, the search for other fabrication techniques is going on. Recent progress in the molecular engineering of polymers has stimulated the development of organic photonics.⁷ Organic structures employing various geometries, such as microdisk, microring, sphere, vertical-cavity surface-emitting, distributed Bragg reflection (DBR), distributed feedback (DFB), and fiber grating, have been used in lasers and amplifiers.⁸⁻¹¹ One problem often encountered in designing organic LD and LED structures is the inherent absence of mirrors, which would be valuable for providing positive feedback for the lasing (in semiconductor structures, cleaved facets of the sample usually play this role). Although this problem can be partly solved by using DFB and DBR structures,⁹ the emission efficiency is still unsatisfactory. Therefore, it is interesting to investigate whether or not the use of PhC mirrors can improve the efficiency of organic photonic devices. Despite the promise of organic PhC structures, realization of them is technically difficult, and with few exceptions has not been addressed in the literature.^{12,13}

Earlier, we investigated the possibility of fabricating organic PhC structures in resins using femtosecond laser mi-

crofabrication. The fabrication of a log-pile three-dimensional (3D) PhC structure employed resin photopolymerization induced by the two-photon absorption (TPA) of tightly focused, powerful femtosecond laser pulses.¹² The structure obtained exhibited significant photonic band gap (PBG) effects. Encouraged by this, we extended our studies to the formation of planar microcavities by introducing defects into the log-pile PhC, and we report the results in this letter. We have observed pronounced cavity resonance modes in our structures, indicating the potential applicability of organic PhC microcavities in light emitting devices.

Our fabrication of polymeric PhC structures was similar to that reported previously.¹² Femtosecond laser pulses were tightly focused inside liquid resin, which is transparent to pulses below the TPA threshold power density. The pulse intensity was adjusted so that the light power density at the focal spot of the laser beam exceeded the TPA threshold, and strong absorption in this highly spatially localized region resulted in photopolymerization of the resin. By scanning the coordinates of the focal spot, predesigned patterns were recorded in the liquid resin. The wavelength and temporal width of the laser pulses used for the fabrication were 400 nm and 150 fs [full width at half maximum (FWHM)], respectively, and the pulse repetition rate was 1 kHz. The laser was focused by a microscope objective with 100 \times magnification and a numerical aperture (NA) of 1.35. A commercially available photopolymer, Nopcure 800 (San Nopco), was used for fabrication. Laser irradiation rendered the exposed regions insoluble, while unexposed regions were dissolved in acetone and removed during the postprocessing stages.

Figure 1(a) shows schematically the structure remaining after the removal of unsolidified resin. This type of periodic 3D structure is commonly known as a log pile, and it consists of horizontally stacked layers of parallel rods, with periodically varying rod orientation and horizontal displacement (period: four layers). The structure fabricated consisted of 20 layers of rods. A planar defect was introduced by removing every other rod from the 10th layer, which was lo-

^{a)}Electronic mail: misawa@eco.tokushima-u.ac.jp

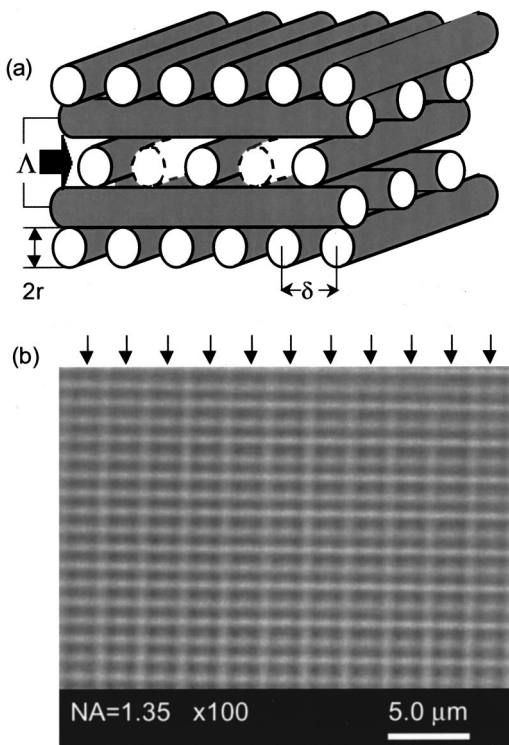


FIG. 1. Schematic of the log-pile structure (a) and optical micrograph of the layer with the defect (top view) in the log-pile PhC (b).

cated in the middle of the PhC structure. Removal was accomplished by simply closing the laser beam while drawing the particular lines. We want to emphasize here the flexibility of direct laser writing for 3D fabrication compared to other techniques, such as holographic lithography, self-organization, and semiconductor processing. Arbitrary defects can be introduced at desired locations without difficulty. This technique also allows easy fabrication of PhC waveguides. However, as the first step, we chose the missing rod planar defect, which has already been demonstrated to exhibit microcavity features in semiconductor PhCs.^{3–5}

Figure 1(b) shows an optical micrograph of the layer with a defect. The arrows indicate the positions of missing rods. Since the top view image presented does not reveal 3D features, we note here that the 3D character of laser micro-fabricated log-pile PhCs in resin was confirmed earlier by scanning electron microscopy.¹² The threshold exposure for polymer solidification depends on the photon fluence, the TPA cross section, the quantum efficiency of the initiator molecules, the chain length, and the branching ratio in the polymerization. The TPA photopolymerization threshold in Nopocure-800 was found to be $\sim 0.2 \mu\text{J}$ under the focusing used,¹⁴ and the rod diameters could be tuned down to sub-diffraction size by carefully adjusting the exposure to slightly above the threshold. The penetration depth depends weakly on the pulse energy because of negligible linear absorption and because of reduced Rayleigh scattering for longer wavelengths. Therefore, photopolymerization via TPA should allow the recording of much thicker structures (hundreds of micrometers) than is possible with the single-photon process.¹⁵ TPA also allows increased spatial resolution, which is required in the fabrication of photonic crystals with PBG in the visible range.¹² The log-pile PhC shown in Fig.

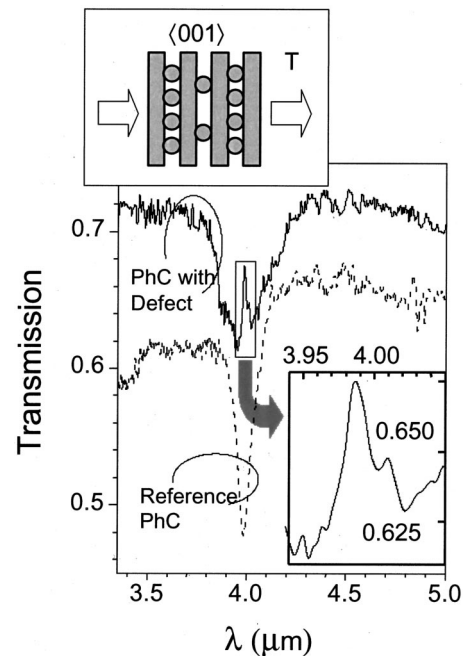


FIG. 2. Measured transmission spectra of the reference PhC without defects (dashed line, offset by -0.1 for clarity) and PhC with a defect. The top inset illustrates the direction of the light propagation in transmission measurements, and the bottom inset shows a detailed view of the defect peak.

1(b) has a rod diameter $2r \sim 0.8 \mu\text{m}$ (assuming a cylindrical rod shape), an in-plane period $\delta \sim 1.3 \mu\text{m}$, and a rod length $L \sim 40 \mu\text{m}$. For the PBG midgap wavelength $\lambda_M \approx 4.0 \mu\text{m}$ determined as described below, the geometric thickness of the defected layer $2r \sim 0.8 \mu\text{m}$ is somewhat smaller than $\lambda_M/2$, indicating that localized modes will significantly penetrate into the PhC mirrors.

To reveal the signatures of PBG and cavity states, the optical transmission of the PhC sample was investigated using a Fourier-transform infrared (FTIR) spectrometer combined with a microscope imaging system. Figure 2 shows the transmission spectra of the investigated sample with a defect (solid line) and the reference sample without a defect (dashed line) for unpolarized light along the $\langle 001 \rangle$ stacking direction. In both samples, the effects of residual absorption were compensated for by normalizing the measured spectra to the absorption spectrum of a uniform photopolymerized material. In the reference sample, a pronounced transmission dip at $3.98 \mu\text{m}$ with a spectral width of approximately 91 nm (FWHM) is seen. The dip magnitude also implies the existence of a photonic pseudogap rather than full PBG in this structure, as can be expected in the case of a relatively low refractive index contrast (about $1.6-1$). This expectation is also confirmed by our numeric simulations (see the description below). In spite of the incomplete PBG, signatures of evolving defect modes can nevertheless be seen in the sample with a defect. The transmission spectrum of this sample reveals a similar, but slightly broader, PBG transmission dip at the same spectral position, and a pronounced transmission peak within it. The physical origin of the peak can be explained roughly in terms of multiple reflections of light between two PBG mirrors surrounding the layer with the defect and forming a planar microcavity. Hence, the peak marks the formation of the microcavity resonance. Light

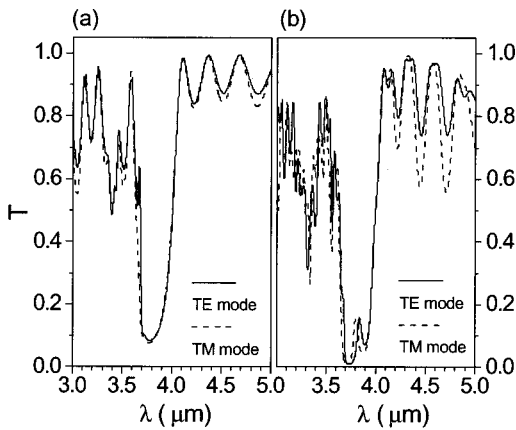


FIG. 3. Simulated transmission spectra for the reference (a) and log-pile PhC with the defect (b) structures.

trapping by the cavity is usually characterized by the quality factor $Q = \omega_0 E / P$, where E is the energy stored in the cavity, ω_0 is the resonant frequency, and $P = dE/dt$ is the dissipated power. The transmission data allow us to estimate the quality factor using the expression $Q = \lambda_R / \Delta\lambda \approx 130$, where λ_R and $\Delta\lambda$ are the peak center wavelength and width, respectively, assuming measured values of $\Delta\lambda = 29.8$ nm (FWHM) and $\lambda_R = 4.01$ μm . It is helpful to note here that semiconductor microcavities formed from high-refractive-index materials may have quality factors as high as 1600.¹⁶ In our case, the relatively low Q value means that the planar defect locally perturbs the light modes at the midgap, but their spatial spreading and escape from the defected region are also significant.

Formation of the PBG and microcavity resonance were also confirmed by numeric modeling. Figure 3 shows the transmission spectra of the reference sample and the sample with the defect, calculated using the transfer-matrix technique.¹⁷ The model structure shown in Fig. 1(a), with measured values of parameters $(r, \delta) \sim (0.4, 1.3)$ μm and refractive index of rods $n = 1.6$, was used for the calculations. Transmission for the transverse electric (TE) (broken line) and transverse magnetic (TM) (solid line) linearly polarized modes was considered separately in anticipation that the absence of some oriented rods in the sample with the defect would result in different conditions for the propagation of TE and TM modes. The calculated transmission spectrum of the reference sample is shown in Fig. 3(a). The spectral positions of the calculated transmission dips are close to those observed experimentally, but the calculated dips are somewhat deeper and broader (the gap to midgap ratio is about 9%). A similar result was obtained for the sample with the defect [Fig. 3(b)], but in this case a distinct peak within the dip marking the microcavity resonance is seen for each polarization. The peaks were centered at 3.801 (TM) and 3.838 μm (TE), and they had Lorentzian line shapes and almost identical amplitudes (about 16%) and Q factors (about 85). As

expected, there was a slight displacement between the peaks of different polarizations due to the anisotropic nature of the defect. Altogether, the numeric simulations qualitatively reproduced the experimental data. The simulations routinely yielded PBG at slightly shorter wavelengths than the measured ones. This is likely to be related to our assumption about the cylindrical shape of the rods, whereas in reality they might be oval shaped, with a slight elongation along the layer-stacking direction, resulting in a higher lattice constant and scaling up of the PBG center wavelength. The elongation may be explained by the fact that the diffraction-limited size of the focal spot along the recording beam propagation (coincident with the layer-stacking direction), $\Delta_{z,y} = 2n\lambda/\text{NA}^2$, is larger than that in the perpendicular plane $\Delta_{x,y} = 1.22 \lambda/\text{NA}$.

In conclusion, we have fabricated and characterized a prototype of planar microcavity, formed by two log-pile polymeric PhC mirrors. The fabrication technique used allows easy tailoring of the structure and introduction of arbitrary defects into it. Despite the fact that the refractive index of the polymerized resin used in the PhC mirrors is insufficient for achieving full PBG, the structure reveals clear signatures of cavity mode formation, and may be considered as a step toward the realization of polymer-based light emitters in the future. The refractive index contrast may be increased by using other initial materials, or by using the polymeric structures fabricated as templates for subsequent in filling by high-refractive-index materials.

¹E. Yablonovitch, Phys. Rev. Lett. **58**, 2059 (1987).

²S. John, Phys. Rev. Lett. **58**, 2486 (1987).

³J. D. Joannopoulos, P. R. Villeneuve, and S. Fan, Nature (London) **386**, 143 (1997).

⁴J. S. Foresi, P. R. Villeneuve, J. Ferrera, E. R. Thoen, G. Steinmeyer, S. Fan, J. D. Joannopoulos, L. C. Kimerling, H. I. Smith, and E. P. Ippen, Nature (London) **390**, 143 (1997).

⁵M. Tokushima, H. Kosaka, A. Tomita, and H. Yamada, Appl. Phys. Lett. **76**, 952 (2000).

⁶V. I. Kopp, B. Fan, H. K. M. Vithana, and A. Z. Genack, Opt. Lett. **23**, 1707 (1998).

⁷J. Huang, K. Yang, Z. Xie, B. Chen, H. Jiang, and S. Liu, Appl. Phys. Lett. **73**, 3348 (1998).

⁸M. Kuwata-Gonokami, R. H. Jodan, A. Dodabalapur, H. E. Katz, M. L. Schilling, R. E. Slusher, and S. Ozawa, Opt. Lett. **20**, 2093 (1995).

⁹M. Nagawa, M. Ichikawa, T. Koyama, H. Shirai, Y. Taniguchi, A. Hongo, S. Tsuji, and Y. Nakano, Appl. Phys. Lett. **77**, 2641 (2000).

¹⁰K. Kuriki, T. Kobayashi, N. Imai, T. Tamyra, S. Nishihara, Y. Nishizawa, A. Tagaya, Y. Koike, and Y. Okamoto, Appl. Phys. Lett. **77**, 331 (2000).

¹¹A. Tagaya, Y. Koike, T. Kinoshita, E. Nihei, T. Yamamoto, and K. Sasaki, Appl. Phys. Lett. **63**, 883 (1993).

¹²H.-B. Sun, S. Matsuo, and H. Misawa, Appl. Phys. Lett. **74**, 786 (1999).

¹³B. H. Cumpston, S. P. Ananthavel, S. Barlow, D. L. Dyer, J. E. Ehrlich, L. L. Erskine, A. A. Heikal, S. M. Kuebler, I.-Y. S. Lee, D. McCord-Maughon, J. Qin, H. Röckel, M. Rumi, X.-L. Wu, S. R. Marder, and J. W. Perry, Nature (London) **398**, 51 (1999).

¹⁴H.-B. Sun, T. Kawakami, Y. Xu, J.-Y. Ye, S. Matsuo, H. Misawa, M. Miwa, and R. Kaneko, Opt. Lett. **25**, 1110 (2000).

¹⁵M. Campbell, D. N. Sharp, M. T. Harrison, R. G. Denning, and A. J. Turberfield, Nature (London) **404**, 53 (2000).

¹⁶J. M. Gerard, D. Barrier, J. Y. Marzin, R. Kuszelewicz, L. Manin, E. Costard, V. Thierry-Mieg, and T. Rivera, Appl. Phys. Lett. **69**, 449 (1996).

¹⁷J. B. Pendry, J. Mod. Opt. **41**, 209 (1994).